Journal of Magnetic Resonance 196 (2009) 127–132

Contents lists available at ScienceDirect

Journal of Magnetic Resonance

journal homepage: www.elsevier.com/locate/jmr

Short, shaped pulses in a large magnetic field gradient

C. Coarna, B. Newling *

UNB MRI Centre, Department of Physics, University of New Brunswick, 8 Bailey Drive, PO Box 4400, Fredericton, NB, Canada E3B 5A3

ARTICLE INFO

Article history:
Received 31 July 2008
Revised 22 October 2008
Available online 31 October 2008

Keywords:
Magnetic resonance imaging
Slice selection
Shaped pulses
Inhomogeneous fields
Stray field
Mobile NMR
Unilateral NMR

ABSTRACT

A number of materials MR developments require that measurements be made in a large magnetic field gradient, including unilateral (single-sided) magnet designs for portability and open access. In such cases, all radiofrequency (RF) pulses are slice selective. Typically, little effort is made to tailor the shape of the selected slice, because shaped RF excitations are viewed as too lengthy in duration to be useful in materials MRI, where signal lifetimes are mostly less than 1 ms. We compare measured magnetization responses to various standard shaped pulses under extreme conditions of application (~30 μs duration, offset frequencies up to 0.3 MHz, and in the presence of a 13 T/m permanent magnetic field gradient). We discuss the feasibility of their implementation for materials MRI in a large gradient, including the difficulty of choosing optimized pulse area, and propose viable solutions.

1. Introduction

In materials MRI, the need for spatial resolution despite the short signal lifetimes of solid and semisolid materials may be met by the use of large magnetic field gradients applied over a small time interval. This strategy, one of several possible [1], has led to several MRI methodologies in which RF excitations must be carried out in the presence of a considerable magnetic field gradient [2,3]. STRAY FIeld Imaging (STRAFI) is one example of a high spatial resolution magnetic resonance imaging technique (~10 μm) for solids and other systems with short T_2 (<1 ms), which uses the constant, stable, high magnetic field gradients existing in the fringe field surrounding a conventional superconducting magnet [4]. Permanent magnets designed with a constant magnetic field gradient can also offer large, stable magnetic field gradients on the order of tens of tesla per meter [5] for STRAFI-like imaging. Perhaps most important, is the widespread use of application-specific magnet designs for portability and open access [6]. In particular, unilateral magnet designs may include incidental [7] or deliberate magnetic field gradients [8,9]. The consequent spread in resonant frequencies, across even a modestly sized sample, is enormous and every RF pulse applied is spatially selective. Depending on the design of the polarizing field, the pulse may select a "sensitive spot" [10] or a more conventional slice [9]. We will use the term "slice" throughout for brevity, although the results presented here are equally, or even more, relevant to the sensitive spot case. Typically, little effort is made to tailor the frequency bandwidth of the selected region, conventional slice selection methods being deemed too lengthy for use with short T_2 materials. Rectangular (constant amplitude) RF pulses are usually employed for excitation. The profile of the selected slice is therefore sinc-like, with a rounded-central maximum and several appreciable, adjacent, out-of-slice maxima (Fig. 1(a)).

In this paper, we argue that it is not difficult to select a carefully tailored slice with conventional, amplitude modulated pulses in materials with intermediate T_2 (0.15–1 ms) in which unilateral and STRAFI methods have hitherto found most application, such as elastomers, semisolids and confined fluids [4,6,11]. While excitation with shaped RF pulses is hardly novel, their use has been dismissed in large magnetic field gradient imaging applications [11]. Several ingenious solutions to the problem of slice selection in very short T_2 materials have been proposed [12,13] including analytical T_2 compensation [14], but we demonstrate that shaped RF pulses are useful in a more brute force sense in MRI of materials with intermediate T_2, by testing them at short durations (~30 μs), over a wide range of offsets (±300 kHz) and in a large static magnetic field gradient (ca. 13 T/m).

There are three separate circumstances, in large gradient applications, under which there are compelling reasons to prefer an RF excitation which engenders a uniform excitation with a sharply defined bandwidth (an *ideal* slice).

(1) A typical strategy for imaging of extended samples in a permanent gradient is to acquire signal slice-by-slice, either by mechanically moving the sample or by sweeping the resonant frequency [4,7]. A simple profile is built up, one slice at a time, without Fourier transformation. An RF excitation

* Corresponding author. Fax: +1 506 453 4581.
E-mail address: bnewling@UNB.ca (B. Newling).

1090-7807/$ - see front matter © 2008 Elsevier Inc. All rights reserved.
doi:10.1016/j.jmr.2008.10.017

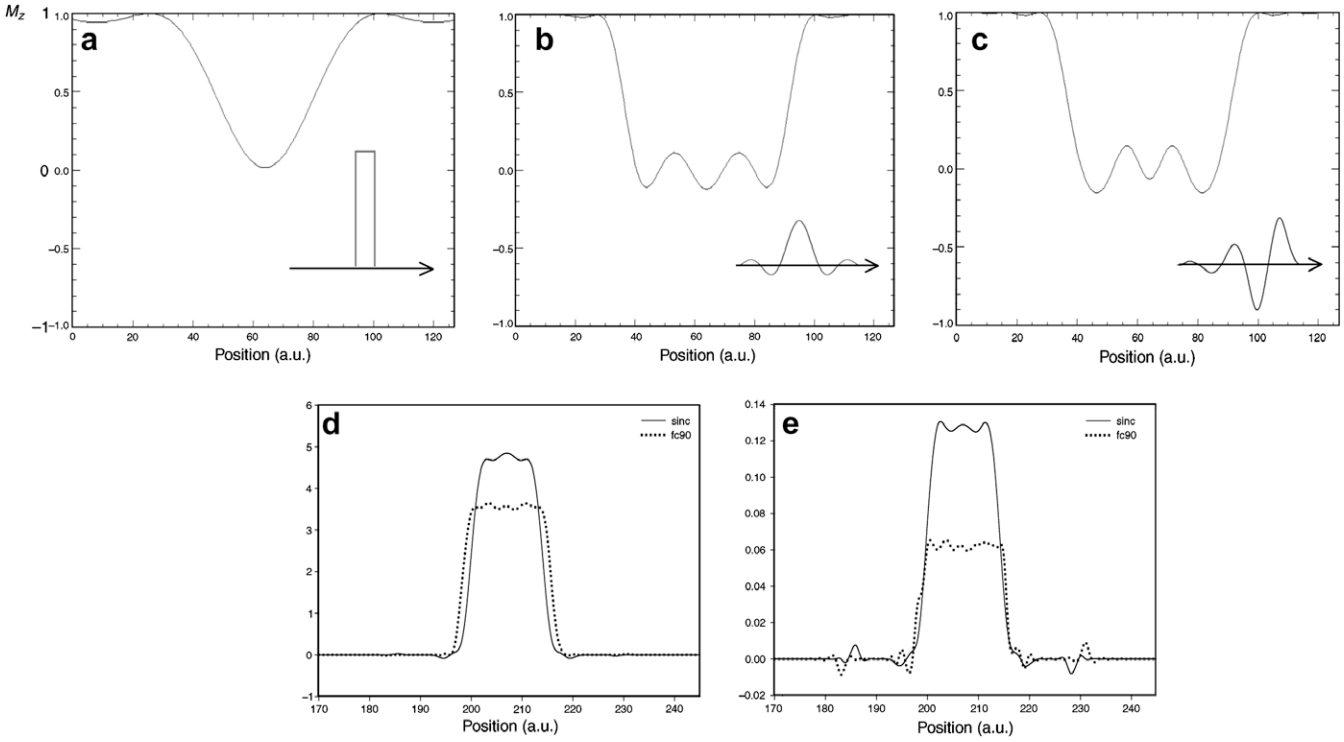

Fig. 1. (a–c) Simulated responses of the magnetization along the axis (z) of the polarizing magnetic field, in the presence of a magnetic field gradient, which renders the frequency-selective pulse spatially selective (*slice* selective). Responses to (a) rectangular amplitude modulation of RF, (b) sinc modulation, (c) fc90 modulation. The tip angle is 90° in each case. The insets show the time domain, amplitude modulated pulse shapes for each excitation. (d and e) Fourier transforms of simulations of the echoes (TE = 180 μs) formed with sinc and fc90 pulses for a material with: (d) T_1 = 340 ms, $T_2 = T_{1\rho}$ = 100 μs, (e) T_1 = 340 ms, $T_2 = T_{1\rho}$ = 30 μs.

such as that of Fig. 1(a), which significantly disturbs the magnetization outside each slice, necessitates a TR between excitations sufficiently long ($5T_1$) to allow the recovery of equilibrium magnetization in order to avoid position dependent T_1-weighting.[1] When an ideal slice is selected, adjacent slices may be interrogated immediately.

(2) When the excited slice encompasses the whole sample (or that part of the sample which is of interest) [4,11,15], uniform excitation is necessary for the profile to give geometrically correct information.

(3) When accurate relaxometry is to be carried out in a large magnetic field gradient or using a unilateral magnet, the excited spins should experience the same RF tip angle, particularly in the case of inversion recovery measurements of T_1 [16].

A *sinc* pulse (whose amplitude is a truncated $\sin(\pi x)/(\pi x)$ function) and the *fc90* pulse [17] (Fig. 1(b) and (c)) were implemented for imaging in a constant magnetic field gradient of G = 12.9 T/m. The fc90 pulse is a self-refocusing pulse shape of similar design to the BURP family of pulses [18] and to their T_2-compensated cousins the SLURP pulses [19]. The fc90 shape was chosen because of the rectangular excitation profile with virtually no out-of-slice excitation. The self-refocusing property of this pulse is also, in principle, attractive, because in a permanent gradient there can be no application of a refocusing gradient lobe (although see below). The sinc pulse is time-symmetric, its point of action being at the center of the pulse application, while the fc90 pulse causes only small excursions of sample magnetization from the longitudinal axis until the end of its application.

Bloch equation simulations of the magnetization responses at the culmination of rectangular, sinc and fc90 pulses are compared in Fig. 1. The effects of relaxation are only included in simulations (d) and (e), which are Fourier transformations of simulated echoes formed with sinc and fc90 pulses.

The product of pulse duration (*pw*) and excitation bandwidth (*BW*) of the slice selected by the three pulses: rectangular, sinc and fc90 is 1, 6 and 6, respectively. The bandwidth is the full width, measured at half maximum amplitude (FWHM) of the slice shape.

A large magnetic field gradient or highly inhomogeneous field typically makes T_2^* shorter than the dead time of the RF receiver hardware and measurements are made using echoes rather than free induction decays. For a given permanent G, resolution in a slice-by-slice profile is primarily determined by the frequency bandwidth (*BW*) of the pulse, which is inversely proportional to the pulse duration (*pw*). The limit to resolution (the largest possible value of *pw*) is, therefore, imposed by the fact that the echo time is restricted by T_2 relaxation [4]. It is the desire for spatial resolution, which limits the use of amplitude modulated pulses to systems with T_2 > ca. 0.15 ms. The phase dispersion at the end of the sinc and rectangular pulses are refocused by the use of echoes, which negates the self-refocusing advantage of the fc90 pulse. However, unilateral magnets with sufficient B_0 homogeneity to acquire an FID have recently become available [10] and there are, therefore, prospects for the use of self-refocusing pulses in FID acquisitions, even in inhomogeneous fields, to eliminate phase dispersion across the selected region.

2. Experimental section

The echo trains were obtained with an Apollo spectrometer (Tecmag, Texas, USA), an AMT M3205A 300-W RF amplifier (American Microwave Technologies, California, USA) and the

[1] An alternative is to acquire non-adjacent slices consecutively [4], which can be prohibitive in acquisition time when mechanical sample repositioning is used.

*open*GARField magnet (Laplacian Ltd., Oxon, UK). The sensitive upper plane of the magnet is characterized by a gradient to magnetic flux density ratio $G/B = 16.6\ \mathrm{m}^{-1}$ at 33.0 ^{1}H MHz. The gradient, G, is 12.9 T/m and is extremely linear in the region between the two shaped pole pieces of a permanent magnet [5]. A home-built surface coil with a square shape (1 mm × 1 mm) and a frequency of 33.1 MHz was used. The bandwidth of the coil (FWHM) is 0.9 MHz (ca. 1.8 mm). Two phantom samples were made from silicone adhesive putty (Clear Silicone, Radiator Specialty Comp, Ontario, Canada): a large phantom extending far beyond the coil and a small phantom within the dimensions of the coil. A leveling phantom was made from poster adhesive (HoldIt, Dixon, Ontario, Canada) pressed on top of a glass microscope slide in order to present a planar surface. A layered sample was prepared from a microscope slide, cover slips and silicone sealant. The relaxation times for silicone were: $T_1 = 340$ ms and $T_2 = 5.4$ ms. The dwell time was 1 μs and the filter width 500 kHz.

3. Results and discussion

The pulse length for a rectangular pulse of nominal tip angle 90° was first determined by the method of Benson and Mc Donald [20] using the quadrature echo pulse sequence 90_x–τ–$(90_y$–τ–echo–τ–$)_n$. The first three echoes following these pulses should have amplitudes in the ratio 1:3/2:3/2, if the duration for a 90° pulse is set correctly. The 90° pulse duration is not that at which maximum signal is obtained. At the maximum amplifier power output used (250 W average), the rectangular 90° pulse duration was 2.5 μs for the extended phantom sample (larger than the dimensions of the coil) and 1.9 μs for the small sample (which fits within the dimensions of the coil).

To set the duration for sinc and fc90 pulses of tip angle 90°, it was necessary to consider the Fourier transform of the echoes, which is the profile of the selected slice. Pulse durations were adjusted to optimize the slice profile, so that it most closely approached the ideal. The optimized 90° pulse duration did not, in

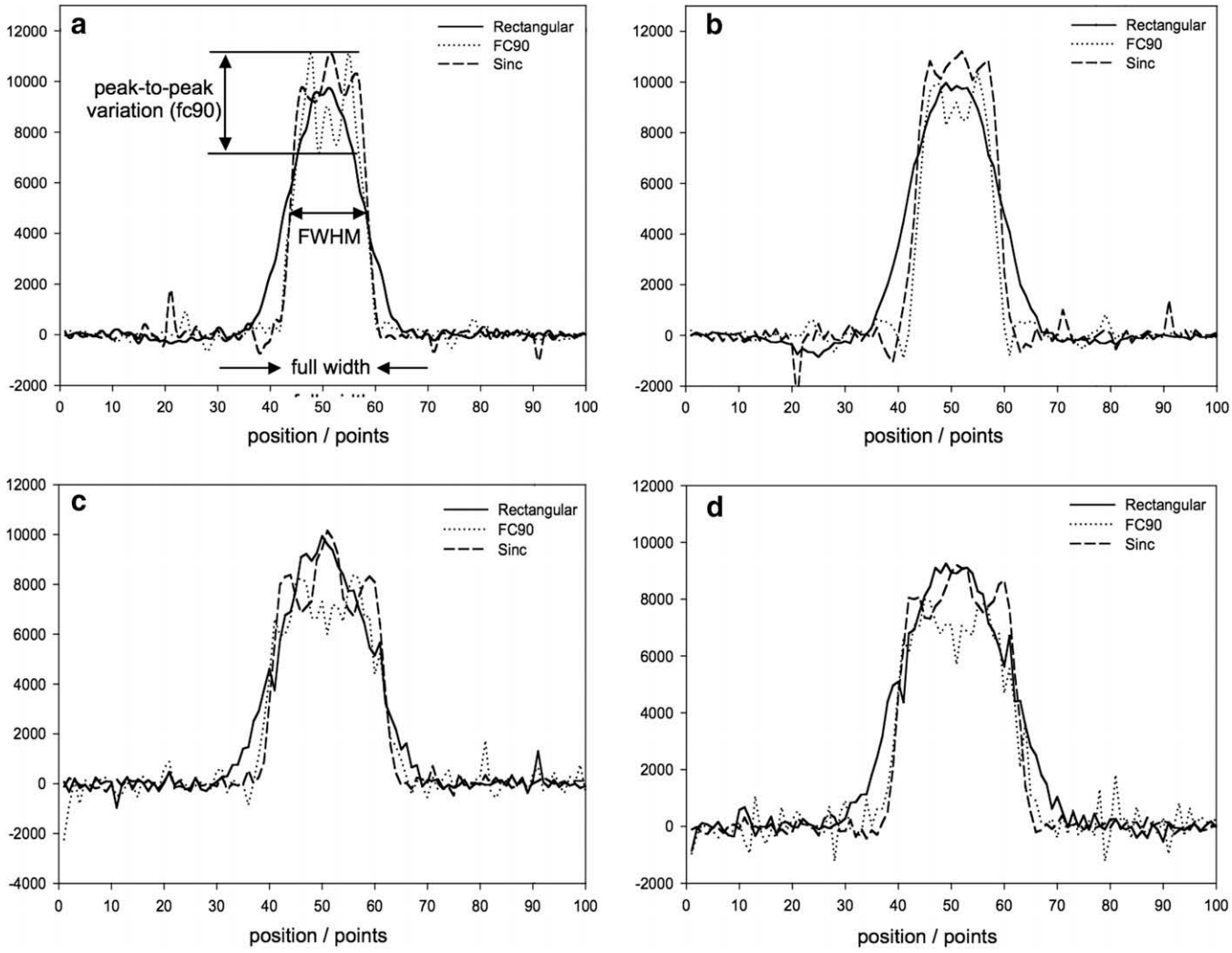

Fig. 2. (a and b) Profiles of the excited slice using an extended sample, larger than the dimensions of the RF coil. Fourier transforms of (a) first echo, (b) eighth echo. In each case, the vertical axis is intensity of magnetization response in arbitrary units and the points in the position axis are separated by 20 μm. Slices shown (bandwidth 193.5 kHz ≡ 352 μm) were selected by the fc90 pulse (duration 31 μs, 1 dB transmitter attenuation), the sinc pulse (31 μs, 8 dB) and the rectangular pulse (5.17 μs, 6 dB and 85% of the fc90 amplitude). Trains of eight echoes were acquired with 128 signal averages, 180 μs echo time (TE) and 100 μs acquisition interval/100 points. The repetition time (TR) was 2 s and the total measurement time was 9 min. The ratio of echo amplitudes for the first three echoes was 1.00:1.20:1.10 (±0.03) for the fc90 pulse and 1.00:1.20:1.20 (±0.03) for the sinc pulse. (c and d) Profiles of the excited slice using a sample smaller than the RF coil. Fourier transforms of (c) first echo, (d) eighth echo. Slices shown (250 kHz ≡ 455 μm) were selected by the fc90 pulse (24 μs,1 dB), the sinc pulse (24 μs, 8 dB) and the rectangular pulse (4 μs, 6 dB). Trains of eight echoes were acquired, with 1056 signal averages, TE = 170 and 100 μs acquisition interval/100 points. TR was 2 s and the total measurement time was 34 min.

Table 1
The ratio between the FWHM and full width (at the axis of zero magnetization) measures rounding of each Fourier transformed slice for the extended and smaller phantom samples. The closer the ratio to 1, the closer the slice to ideal (the less rounded the slice profile). The fractional non-uniformity measures the inhomogeneity of excitation across the slice. The smaller the fraction (of maximum slice amplitude), the closer the slice to ideal (more homogeneous excitation).

Pulse	Echo #	FWHM/full width		Fractional non-uniformity	
		Extended sample	Small sample	Extended sample	Small sample
Rectangular	1	0.50	0.58	n/a	n/a
	2	0.57	0.58	n/a	n/a
	3	0.54	0.59	n/a	n/a
	8	0.56	0.56	n/a	n/a
fc90	1	0.70	0.70	0.35	0.27
	2	0.74	0.77	0.28	0.31
	3	0.74	0.73	0.29	0.24
	8	0.78	0.72	0.19	0.28
Sinc	1	0.70	0.81	0.18	0.34
	2	0.73	0.80	0.10	0.21
	3	0.72	0.79	0.12	0.31
	8	0.72	0.76	0.10	0.20

general, correspond to the maximum in acquired echo signal. We found the most robust approach to be use of the CPMG pulse sequence 90_x–τ–$(180_y$–τ–echo–τ–$)_n$ [21] with a 90° rectangular pulse (as determined above) and with a sinc/fc90 180° to determine a first approximation to the 90° sinc/fc90 pulse duration. The final pulse duration was determined by optimization of the slice profile generated with identically shaped 90° and 180° pulses (see below). With 250 W of applied RF power, the 90° pulse duration for the sinc was 12.3 μs for the extended phantom sample (ratio of echo amplitudes for the first three echoes was 1.00:1.20:1.20 ±0.03) and 9.6 μs for the small sample. At the same power, the 90° fc90 pulse was 27.6 μs in duration for the extended sample (ratio of echo amplitudes 1.00:1.20:1.10 ±0.03) and 21.4 μs for the small sample.

To compare the shapes of the selected slice using the three pulses, they were applied with the same bandwidth and echo time in a CPMG sequence, with 90° and 180° pulses identically shaped. For the rectangular and the sinc pulses, the pulse duration for a refocusing tip angle of 180° was the same as the pulse duration for the 90°, but the RF amplitude was doubled, so as to refocus the same bandwidth as that excited [20]. For the fc90 pulse, a refocusing *fc180* pulse (with double the $pw \times BW$ product of the original fc90) was constructed by placing a time-reversed fc90 at the end of a normal fc90 [22]. This is an incidental, but sometimes useful, feature of the self-refocusing pulse, which allows the 90° and 180° pulses to have the same amplitude, while retaining the same bandwidth.

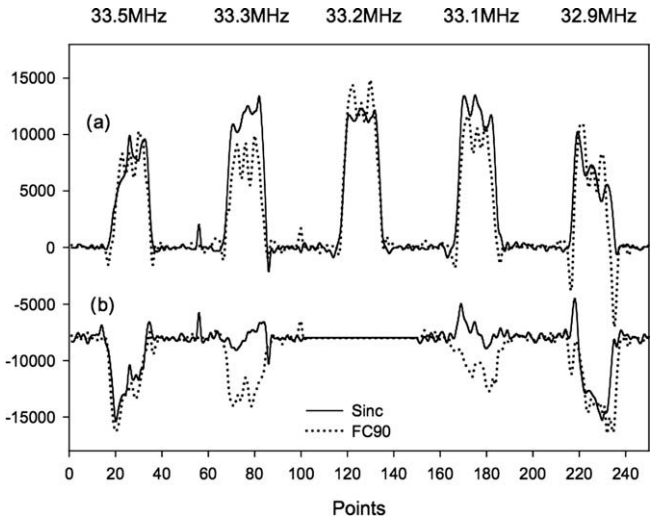

Fig. 3. (a) A comparison of the slice obtained by Fourier transformation of the second echo from CPMG trains of sinc and fc90 pulses, showing frequency dependence. (b) A comparison of the slice residuals calculated by subtracting the profile of the on-resonance slice (33.2 MHz) from the offset slices. Pulse bandwidths were (193.5 kHz) for fc90 (31 μs, 1 dB) and sinc (31 μs, 8 dB) pulses. Trains of eight echoes were acquired with 128 scans; TE = 180 μs and acquisition interval 100 μs/100 points. TR was 2 s and the total measurement time was 9 min. The same acquisitions were made at 33.5, 33.3, 33.2, 33.1, and 32.9 MHz in the extended phantom sample.

In the extended phantom sample, an fc90 pulse with a pulse length of 31 μs at 1 dB (transmitter attenuation), which excited a 193.5 kHz bandwidth, was chosen. To maintain the same bandwidth, the duration for the sinc pulse was 31 μs at 8 dB and for the rectangular pulse was 5.17 μs at 6 dB and 85% of the fc90 amplitude. For all three pulses, trains of eight echoes were acquired, in 128 signal averages. The echo time, TE, was 180 μs and the acquisition interval was 100 μs with 100 digitized complex data points. The repetition time, TR, was 2 s and the total measurement time was 9 min. The comparison is presented in Fig. 2 for the first and eighth echoes of the train.

In the small phantom sample, an fc90 pulse with a pulse length of 24 μs at 1 dB, which excited a 250 kHz bandwidth was chosen. To maintain the same bandwidth the duration for the sinc pulse was 24 μs at 8 dB and for the rectangular pulse was 4 μs at 6 dB. For all three pulses, trains of eight echoes were again acquired, in 1056 signal averages. TE was 170 μs and the acquisition interval was again 100 μs, spanned by 100 digitized points. TR was 2 s and the total measurement time was 34 min. The resonant frequency was 33.2 MHz for sinc and fc90 pulses, and 33.1 MHz for the rectangular pulse (Fig. 2).

For the extended sample there are features at the slice edges in the profiles, which are discussed in the literature [23]. The profile obtained with the rectangular pulse is, of course, the most rounded and shows out-of-slice excitation in Fig. 2(b), despite the filter width of 500 kHz (half of the complete spectral width). For a quantitative comparison of rounding of the slice, the ratio between the

Table 2
A comparison between sinc and fc90 shaped pulses of the ratio of average intensity of the slice obtained by Fourier transformation of the second echo in a CPMG train (Fig. 3(a)) for different frequencies with respect to the resonance frequency 33.2 MHz.

Frequency (MHz)	Ratio of average slice intensity (Fig. 3(a)) to that of the on-resonance slice	
	fc90 ratio	Sinc ratio
32.9	0.63	0.62
33.1	0.79	1.05
33.2	1.00	1.00
33.3	0.64	0.98
33.5	0.63	0.68

width of the slice at the axis of zero magnetization (full width, see Fig. 2(a)) and FWHM for each Fourier transformed slice was calculated for each of the three pulses (Table 1). For a comparison of the uniformity of excitation, the peak-to-peak variation in intensity of MR signal from each slice (Fig. 2(a)) was divided by the maximum intensity to give a fractional measure of non-uniformity in the excitation. The latter figure is meaningless in the magnetization response to the rectangular pulse, which is smoothly rounded from the peak (there is no region of uniform excitation).

As expected, the sinc and fc90 pulse shapes yield slice profiles far closer to ideal (with the FWHM/full width ratio closer to one, indicating less rounding of the slice) than the usual rectangular pulse. The sinc pulse shape outperforms the fc90 pulse in slice selection through the small sample, but there is very little to choose between them in the extended sample. The slice experiences a distribution of flip angles in parts of the sample beyond the dimensions of the coil. Despite this, and despite the naivety of our RF coil design, the fc90 and sinc pulse shapes result in very respectable profiles of an excited slice with very low out-of-slice excitation for extended samples. This is a critical test in open-access magnet designs (such as the *open*GARField), which are important in materials MRI precisely because of their ability to interrogate part of a large sample. The well-controlled, linear gradient of the *open*GARField magnet allows for prototyping of techniques for use in other constant gradient devices, such as portable MR sensors [24].

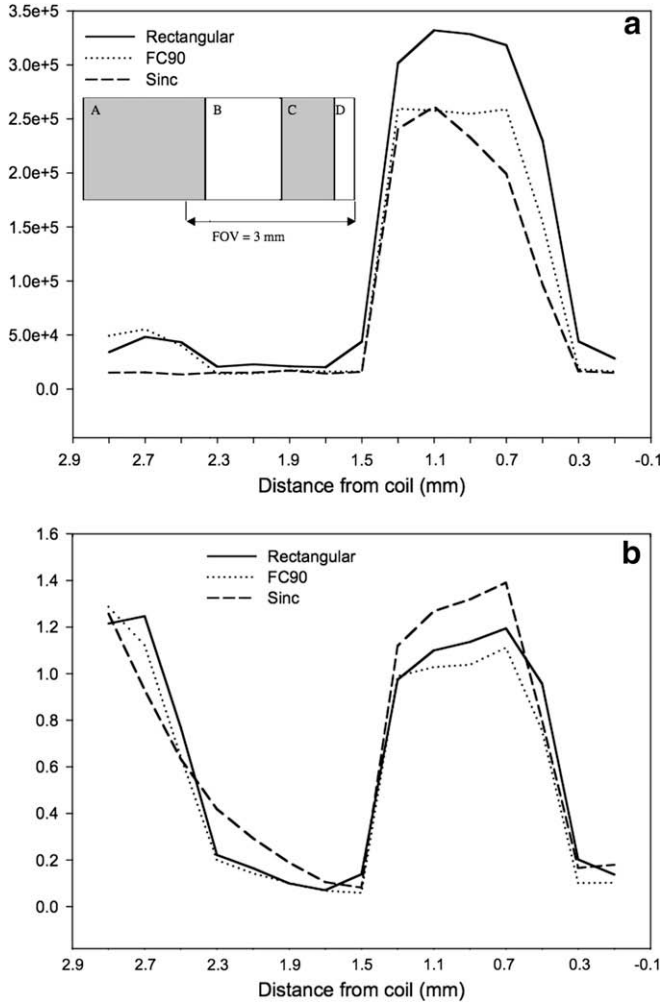

Fig. 4. Profiles of a layered sample. (a) Un-normalized profiles, with (inset) a schematic of the layered sample and the field of view. A = silicone of thickness 2.6 mm; B = glass, 1 mm; C = silicone, 0.85 mm; D = glass, 0.3 mm. The RF coil is beneath the sample (to the right, as drawn). (b) The same profiles, but normalized with respect to a separate *calibration* profile (not shown) of a uniform silicone sample. At each point, the profile is divided by the corresponding value in the calibration profile. The normalized profile is thus corrected for the intensity effects of B_1 inhomogeneity. Fifteen slices were acquired with separations of 0.1 MHz, between 32.4 and 33.8 MHz. Four echoes, 100 acquisition points and 128 scans were acquired for each slice. TE was 25 μs. The durations of the pulses were: 62 μs (7 dB transmitter attenuation) for the fc90 shaped pulse, 62 μs (17 dB) for the sinc pulse and 10 μs (12 dB) for the rectangular pulse (all pulses had the same bandwidth).

Both sinc and fc90 pulses can be employed for a successful slice selection in the 12.9 T/m permanent gradient, at a frequency near the resonant frequency of the coil. Off resonance, the profile of the slice is no longer very rectangular. The frequency response of the RF coil causes the amplitude of the RF excitation to depend on offset (Fig. 3(a)). For the rectangular pulse, the shape of the selected slice does not change significantly with offset frequency. Self-refocusing pulses, such as the fc90 shape, are designed with a specific tip angle in mind (in the case of fc90, the intended tip angle is 90°) and cannot, in general, be applied at arbitrary amplitude to give arbitrary excitation tip angle across the selected slice. The fc90 pulse might be expected to be unsuitable, therefore, for swept frequency applications. The response of the spin system is sufficiently linear, however, that the sinc pulse may be used successfully for slice selective excitations of arbitrary tip angle [25]. In Fig. 3, the offset selected slices for the fc90 and sinc pulse shapes are compared. The lower line shows, for each offset frequency, the difference between the selected slice and that at 33.2 MHz (on resonance). At 0.300 MHz offsets there is, rather surprisingly, little to choose between the sinc and fc90 slice profiles. At 0.100 MHz offsets, the fc90 slice profiles are considerably more attenuated than their sinc-excited counterparts (see Table 2). However, the uniformity of excitation in the sinc slice profiles is as bad, if not worse, than the fc90 profiles, showing an exaggerated slope towards the on-resonance frequency.

The effects of relaxation upon the slice selection of shaped pulses are the principle reason cited for their non-use in materials MRI. In simulation (Fig. 1(d) and (e)), the effects upon slice selection are shown to be mostly in signal amplitude, rather than in slice shape, even when the simulated T_2 of the sample is equal to the shaped pulse duration (Fig. 1(e)). The amplitude units on the vertical axis are arbitrary, but consistent, and show the effect of T_2 relaxation upon slice signal amplitude (in Fig. 1(e), TE is six times longer than T_2). In echo formation, the distorting effects of relaxation during RF pulse application are far less important for shaped pulse slice selection in materials MRI than are the simple effects of signal attenuation during the TE interval.

In order to compare the performance of the pulses when profiling a layered sample by sweeping the frequency, identical CPMG sequences were applied for each of the three pulses. The scheme of the layered sample and the field of view used (being limited by the construction of our RF coil) are shown in the inset of Fig. 4(a). Fifteen slices, with separations of 0.1 MHz, between 32.4 and 33.8 MHz were acquired. Four echoes, 100 acquisition points and 128 scans were acquired for each slice. The echo time was 25 μs. Profiles were constructed by summation of all four echoes and recording the echo maximum at the position corresponding to the appropriate frequency offset in the 12.9 T/m gradient (Fig. 4(a)). The profile was normalized with respect to a reference profile acquired in the same conditions but using an extended, uniform sample of silicone (Fig. 4(b)).

Sinc pulse excitation leads to a rounding (blurring) of the sample profile at the extremity of the coil response (more than 2.0 mm from the coil). This is rather unexpected, given the satisfactory performance of the sinc pulse in slice selection above. Notice that the range of excitation frequencies represented in Fig. 4 is greater than trialed in Fig. 3. Even in the un-normalized profile (Fig. 4(a)), it is apparent

that the sinc pulse affects no excitation in the leftmost silicone layer (A in the inset). This effect is, of course, duplicated in the calibration profile, so that the normalized sinc profile (Fig. 4(b)) shows exaggerated blurring, where one noisy signal is divided by another. The fc90 and rectangular pulses show a greater useful frequency range and lead to more faithful sample profile. There is little to choose between the two profiles, but the absence of out-of-slice excitation with use of the fc90 pulse allows the potential for more rapid excitation of adjacent slices as detailed above.

4. Conclusion

Conventional shaped (amplitude modulated) RF pulses, played out in tens of microseconds, represent a viable alternative to rectangular pulses in materials MRI in large magnetic field gradients. Well-defined slice selection is an asset for slice-by-slice profiling in a permanent gradient, Fourier transform profiling or relaxometry. With a view particularly to application in unilateral magnets, short, sinc-shaped and self-refocusing (fc90) pulses were compared with rectangular excitation in a larger gradient (12.9 T/m) and over a wider range of offsets (±300 kHz centered at 33.2 ^{1}H MHz) than previously reported. With careful calibration of pulse amplitude, both sinc and fc90 pulses gave satisfactorily well-defined slice excitation in a sample smaller than the RF coil and in a sample which extends beyond the geometry of the coil. The latter case is typical of open magnet geometry applications. Our open magnet has an unusually linear magnetic field gradient, but some recent open, portable magnet designs also have well-defined magnetic field gradients [9], which suggest the use of slice selective pulses in imaging, as demonstrated herein.

We note that the maximum in echo signal amplitude does not in general indicate an optimal choice of pulse amplitude for slice selection and that the ratio of amplitudes in an echo train is different for differently shaped pulses. This observation is in accord with those previously made for rectangular pulses [20]. Just as for rectangular pulses, the ratios of CPMG echo amplitudes for the sinc (1.00:1.20:1.20) and fc90 pulses (1.00:1.20:1.10) will now be used for convenient pulse calibration.

In simulation, slice selection by shaped RF pulses is compromised only when $T_2 \leqslant$ pulse duration and the shaped pulse duration can be as short as 30 μs on standard equipment (including a home-built RF coil and a 300 W RF amplifier). However, a pulse duration of 30 μs *does* impose a minimum possible TE (ca. 150 μs on our equipment): this has a greater effect upon the usefulness of standard shaped pulses in very short T_2 materials than does any loss of selectivity due to relaxation during the pulse itself. In intermediate T_2 materials (T_2 = 0.15–1 ms), which still comprise the majority of those studied by materials MRI, the shaped pulse durations are not at all inconvenient. The use of shaped pulses in swept-frequency profiling was demonstrated. The sinc pulse showed a slightly smaller useful frequency range in profiling than the rectangular and fc90 pulses.

There are, of course, many possible variations on the excitations demonstrated here. Many other pulse shapes have been designed and alternative RF coil geometries, for example, may extend the useful frequency range of these selective excitations. No particular attempt has been made to optimize these excitations or the RF hardware for particular circumstances. The viability and robustness of shaped RF excitations for careful slice selection in materials MRI in large magnetic field gradients and extended samples has, therefore, been amply demonstrated.

Acknowledgments

The authors thank the New Brunswick Innovation Foundation (Research Assistantship Awards) and Canada's Natural Science and Engineering Research Council (NSERC) for financial support. B.N. would like to thank Dr. Peter Aptaker of Laplacian, UK for stimulating discussions.

References

[1] B. Blumich, NMR Imaging of Materials, Oxford University Press, Oxford, UK, 2000.
[2] S. Emid, J.H.N. Creyghton, High resolution NMR imaging in solids, Physica B+C 128-1 (1985) 81–83.
[3] I. Chang, G. Hinze, G. Diezemann, F. Fujara, H. Sillescu, Self-diffusion coefficients in plastic crystals by multiple-pulse NMR in large statistic field gradients, Phys. Rev. Lett. 76 (1994) 2523–2526.
[4] P.J. McDonald, B. Newling, Stray field magnetic resonance imaging, Rep. Prog. Phys. 61 (1998) 1441–1493.
[5] P.M. Glover, P.S. Aptaker, J.R. Bowler, P.J. McDonald, E. Ciampi, A novel high-gradient permanent magnet for the profiling of planar films and coatings, J. Magn. Reson. A 139 (1999) 90–97.
[6] B. Blümich, J. Perlo, F. Casanova, Mobile single-sided NMR, Prog. NMR Spectrosc. 52 (2007) 197–269.
[7] J. Perlo, F. Casanova, B. Blümich, Profiles with microscopic resolution by single-sided NMR, J. Magn. Reson. 176 (2005) 64–70.
[8] A.E. Marble, I.V. Mastikhin, B.G. Colpitts, B.J. Balcom, An analytical methodology for magnetic field control in unilateral NMR, J. Magn. Reson. 174 (2005) 78–87.
[9] A.E. Marble, I.V. Mastikhin, B.G. Colpitts, B.J. Balcom, A constant gradient unilateral magnet for near-surface MRI profiling, J. Magn. Reson. 183 (2006) 240–246.
[10] A.E. Marble, I.V. Mastikhin, B.G. Colpitts, B.J. Balcom, Designing static fields for unilateral magnetic resonance by a scalar potential approach, IEEE Trans. Magn. 43 (2007) 1903–1911.
[11] P.J. McDonald, Stray field magnetic resonance imaging, Prog. Nucl. Magn. Reson. Spectrosc. 30 (1997) 69–99.
[12] G.J. Galloway, W.M. Brooks, J.M. Bulsing, I.M. Brereton, J. Field, M. Irving, H. Baddeley, D.M. Doddrell, Improvements and extensions to the DIGGER technique for performing spatial selective excitation, J. Magn. Reson. 73 (1987) 360–368.
[13] M.L. Kilfoil, P.T. Callaghan, Selective storage of magnetization in strongly relaxing spin systems, J. Magn. Reson. 150 (2001) 110–115.
[14] D.E. Rourke, L. Khodarinova, A.A. Karabanov, Two-level systems with relaxation, Phys. Rev. Lett. 92 (16) (2004), doi:10.1103/PhysRevLett.92.163003.
[15] P.R. Laity, P.M. Glover, J.N. Hay, Composition and phase changes observed by magnetic resonance imaging during non-solvent induced coagulation of cellulose, Polymer 43 (22) (2002) 5827–5837.
[16] R.R. Ernst, G. Bodenhausen, A. Wokaun, Principles of Nuclear Magnetic Resonance in One and Two Dimensions, Clarendon Press, Oxford, 1987. pp. 119–124.
[17] T.P.L. Roberts, T.A. Carpenter, L.D. Hall, Design and application of prefocused pulses by simulated annealing, J. Magn. Reson. 89 (1990) 595–604;
A.R.C. Gates, T.P.L. Roberts, N.J. Shah, T.A. Carpenter, L.D. Hall, Reduction of flow artifacts in fast gradient-recalled echo imaging by the use of prefocused pulses, J. Magn. Reson. 96 (1992) 222–228.
[18] H. Geen, R. Freeman, Band-selective radiofrequency pulses, J. Magn. Reson. 93 (1991) 93–141.
[19] J.M. Nuzillard, R. Freeman, Band-selective pulses designed to accommodate relaxation, J. Magn. Reson. A 107 (1) (1994) 113–118.
[20] T.B. Benson, P.J. McDonald, Profile amplitude modulation in stray-field magnetic-resonance imaging, J. Magn. Reson. A 112 (1995) 17–23.
[21] T.B. Benson, P.J. McDonald, The application of spin echoes to stray-field imaging, J. Magn. Reson. B 109 (1995) 314–317.
[22] T.P.L. Roberts, T.A. Carpenter, L.D. Hall, A simple method for the construction of 180° refocusing RF pulses for use in nuclear magnetic resonance imaging, J. Magn. Reson. B 101 (1993) 78–82.
[23] M.D. Hürlimann, Diffusion and relaxation effects in general stray field NMR experiments, J. Magn. Reson. 148 (2001) 367–378.
[24] S. Rahmatallah, Y. Li, H.C. Seton, I.S. Mackenzie, J.S. Gregory, R.M. Aspden, NMR detection and one-dimensional imaging using the inhomogeneous magnetic field of a portable single-sided magnet, J. Magn. Reson. 173 (2005) 23–28.
[25] P.T. Callaghan, Principles of Nuclear Magnetic Resonance Microscopy, Oxford University Press, Oxford, UK, 1991.